Paleoceanography and Paleoclimatology

AGU ADVANCING EARTH AND SPACE SCIENCE

RESEARCH ARTICLE
10.1029/2021PA004356

Spatial and Temporal Trends in Mineral Dust Provenance in the South Pacific—Evidence From Mixing Models

Jack Longman[1], **Torben Struve**[1], **and Katharina Pahnke**[1]

[1]Marine Isotope Geochemistry, Institute for Chemistry and Biology of the Marine Environment (ICBM), University of Oldenburg, Oldenburg, Germany

Key Points:

- Bayesian mixture modeling of multi-isotope datasets allows for precise apportionment of mineral dust sources to the South Pacific
- South Pacific mineral dust input from South America was greater during the Last Glacial Maximum (53%) than during the Holocene (31%)
- Modeling individual mineral dust mixtures reveal zonal and meridional gradients in Holocene and Last Glacial Maximum data

Supporting Information:

Supporting Information may be found in the online version of this article.

Correspondence to:

T. Struve,
t.struve@icbm.de

Citation:

Longman, J., Struve, T., & Pahnke, K. (2022). Spatial and temporal trends in mineral dust provenance in the South Pacific—Evidence from mixing models. *Paleoceanography and Paleoclimatology*, *37*, e2021PA004356. https://doi.org/10.1029/2021PA004356

Received 25 AUG 2021
Accepted 20 JAN 2022

Author Contributions:

Conceptualization: Jack Longman, Torben Struve
Data curation: Jack Longman
Formal analysis: Jack Longman, Torben Struve
Investigation: Jack Longman, Torben Struve, Katharina Pahnke
Methodology: Jack Longman
Resources: Katharina Pahnke
Software: Jack Longman
Validation: Jack Longman, Torben Struve
Visualization: Jack Longman, Torben Struve

Abstract Mineral dust is an important component of the Earth system due to its role in oceanic nutrient supply, cloud formation and its radiative properties. Changes in transport pathways and fluxes of mineral dust have attracted increased attention using radiogenic isotope analysis for detailed investigation of changing dust sources through time. However, multi-isotope studies provide complex datasets of dust provenance, often without exact quantification of source contributions. Here we use Bayesian mixing models and existing radiogenic isotope data to quantify changes in South Pacific dust provenance for the Holocene and the Last Glacial Maximum (LGM; ~18–24 ka BP). Testing different model configurations showed grouping small source regions to single continental scale end members prior to modeling can lead to biased results, and so we group model outputs post-modeling. During the LGM, a higher proportion (mean 53%) of dust entering the South Pacific was South American in origin, compared to a Holocene mean of 31%. In contrast, Australian dust contributions were lower during the LGM (mean 38%) than Holocene (mean 55%), with significant spatial gradients for both time slices. In the subpolar South Pacific, the high representation of South American dust during the LGM (up to ~75%) coincides with larger dust particles; together indicating that far-traveled dust transport was facilitated by long atmospheric residence times and an accelerated westerly wind circulation during this time. Our study shows how Bayesian mixing models provide valuable constraints for dust source contributions, an approach which may help in the calibration of atmospheric models, using complex isotopic datasets.

Plain Language Summary Mineral dust can influence the Earth's radiation budget, cloud formation, and the supply of nutrients to marine and terrestrial ecosystems. Southern Hemisphere oceans are of particular interest due to airborne nutrient supply from mineral dust promoting primary productivity. The geochemical fingerprint of dust can help to identify sources and transport pathways of dust in the Southern Hemisphere. Here, we model existing geochemical data to identify changes in dust sources in the South Pacific between the current warm interval (the Holocene) and the peak of the last ice age. Our results show that dust delivered to the South Pacific is generally related to emissions from Australia (dominating during the Holocene) and South America (dominating during the last ice age), with distinct gradients in the distribution of dust across the study area during the two time periods. The ice age dust input coincided with the delivery of larger particles to the study area, indicating dust remained in the atmosphere longer, driven by higher wind speeds in the circumpolar westerly wind system.

1. Introduction

Mineral dust is a vital component of the Earth system (Goudie & Middleton, 2006). By regulating micronutrient supply (Jickells et al., 2005; Mahowald et al., 2005, 2018), changes in mineral dust (here referred to as "dust") transport can affect land and marine ecosystems (Aciego et al., 2017; Boyd et al., 2010; Maher et al., 2010), surface albedo (Painter et al., 2007), influence cloud formation (Karydis et al., 2011) and the energy balance of the Earth via scattering and absorbing incoming solar radiation (Kok et al., 2018; Li et al., 2021; Shao et al., 2013). Nutrients delivered to the marine environment by dust may play a key role in regulating biogeochemical cycles, in particular in remote ocean areas where nutrients may otherwise be limited (Jickells et al., 2005; Moore et al., 2013). This results in increased primary productivity and enhanced carbon export (Pabortsava et al., 2017; Sarmiento & Gruber, 2006), thus reducing atmospheric CO_2 (Jickells et al., 2005; Martin, 1990; Sigman & Boyle, 2000).

Writing – original draft: Jack Longman, Torben Struve
Writing – review & editing: Jack Longman, Torben Struve, Katharina Pahnke

In the Southern Ocean, the role of dust in controlling carbon cycling is profound, with evidence suggesting a coupling between Southern Hemisphere dust, CO_2 and temperature changes during glacial cycles (Jaccard et al., 2013; Lambert et al., 2008; Martin, 1990; Martínez-García et al., 2011, 2014). In the Southern Ocean, availability of the micronutrients iron (Fe) and/or manganese (Mn) are considered important limiting factors for phytoplankton growth (Blain et al., 2007; Browning et al., 2021; Martin, 1990; Smetacek et al., 2012). As such, supply of these nutrients via the deposition of dust may alleviate deficiencies and enhance primary production (Maher et al., 2010; Tagliabue et al., 2017). Such a process would be especially important during glacial periods like the Last Glacial Maximum (LGM; c. 18–24 ka; Maher et al., 2010), when dust input to the Southern Ocean was three times greater than present (Lamy et al., 2014; Martínez-García et al., 2011).

The ability of dust to provide bioavailable Fe depends upon mineralogy, atmospheric transport, and processing of dust by sea-ice and in the water column (Albani et al., 2016; Li et al., 2021; Shi et al., 2012). Consequently, a comprehensive interpretation of the role of dust deposition on the carbon cycle requires knowledge of source areas and transport pathways (Loveley et al., 2017; Shi et al., 2012; Shoenfelt et al., 2018). The isotope compositions of neodymium (Nd), strontium (Sr), and lead (Pb) are powerful source tracers (Grousset & Biscaye, 2005). The size fraction of far-travelled dust (Delmonte et al., 2017; Kok et al., 2017; Mahowald et al., 2014) is also found in lithogenic marine sediments (Erhardt et al., 2021; van der Does et al., 2021; Wengler et al., 2019), which can be used to investigate dust sources and transport in ocean areas where atmospheric input is the exclusive (or at least predominant) source of lithogenic material in this size fraction. This approach has been applied to reconstruct dust provenance in the South Pacific showing a shift from predominantly Australian sources in Holocene times (Wengler et al., 2019) to a stronger contribution from South American sources during the LGM (Struve et al., 2020). However, the published work relied upon simple two end-member mixing models and comparison of data to potential source regions (e.g., Struve et al., 2020; Trudgill et al., 2020; Wengler et al., 2019). Therefore, a more comprehensive approach providing absolute values for source contributions is desirable.

Bayesian isotopic mixing models such as MixSIAR were developed in the biological field to apportion prey contributions to the diet of predators using the isotopic composition of both predator and prey tissue (Parnell et al., 2010, 2013). MixSIAR has previously been applied to the source apportionment of Pb isotopes in pollution reconstructions (Longman et al., 2018) and to sediment provenance (Blake et al., 2018; Huangfu et al., 2020), but only very recently to dust provenance (Erhardt et al., 2021). This is despite the ability of such models to apportion absolute contributions from many sources. An approach that provides robust estimates of shifting source input spatially and temporally will be valuable not only simply to better understand changing sources of dust but also to validate modeling approaches aiming to understand the deposition of dust using general circulation model (GCM) data (e.g., Albani et al., 2012; Lunt & Valdes, 2002), or air mass transport reconstructions (McGowan & Clark, 2008; Neff & Bertler, 2015). Here, we apply MixSIAR in a number of ways to the radiogenic isotope composition of the dust fraction from South Pacific marine sediments to better estimate contributions of various dust sources to the region spatially and temporally. In this study, we emphasize the importance of a critical assessment of the dust compositions in the source regions and considerations of possible transport pathways for the meaningful interpretation of model results.

2. Methods

2.1. Model Outline

For all modeling completed in this work, we utilize the framework of MixSIAR, the latest version in a series of Bayesian mixing models (Stock et al., 2018; Stock & Semmens, 2013). MixSIAR relies upon the following equations, expressed here as a single isotope system with three sources:

$$X_M = f_A X_A + f_B X_B + f_C X_C \quad (1)$$

$$1 = f_A + f_B + f_C \quad (2)$$

where f and X denote the fraction and the isotopic composition, respectively. The subscript "M" denotes the measured signal resulting from the mixture of the sources A, B, and C. Since this is an underdetermined system, with three unknowns and two equations, there is no unique solution. However, combinations of source contributions can be compared to mixture signature to determine potential solutions. By examining model fits developed

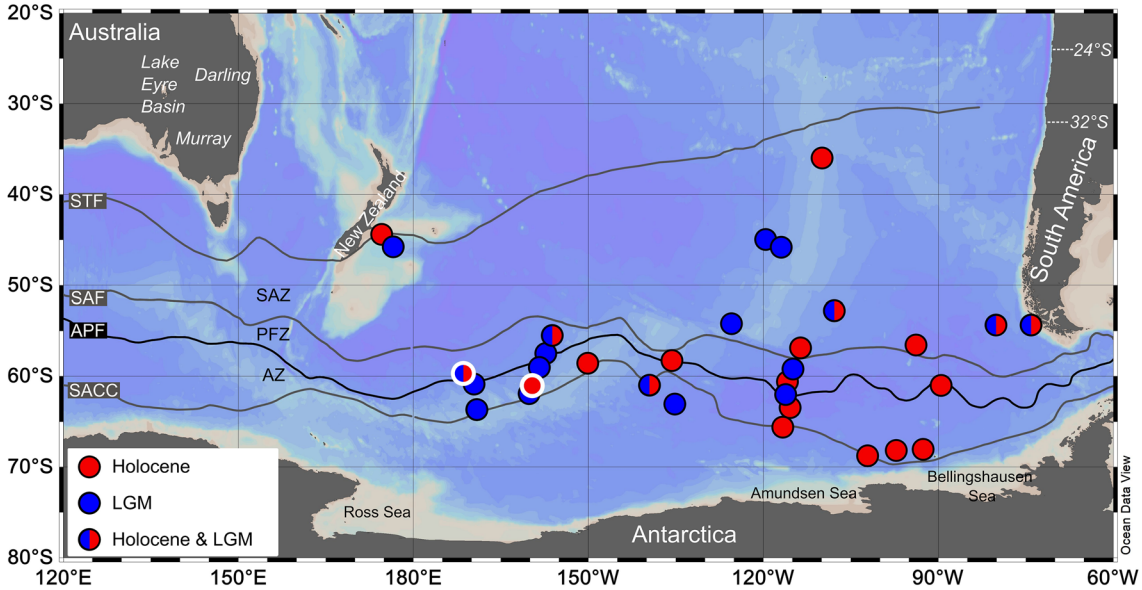

Figure 1. Location of all sites used in this study. Sites with samples of Holocene age only are marked with red circles, whilst sites with only Last Glacial Maximum (LGM) samples are marked by blue circles. Locations with samples from both periods are marked with circles containing red and blue filling. White outline indicates sample locations used for sensitivity tests (see also Table S3 in Supporting Information S1). Dashed white lines at 24°S and 32°S indicate subdivision of South American source areas based on their geochemical composition following Struve et al. (2020). APF, Antarctic Polar Front; AZ, Antarctic Zone; SACC, Southern ACC Front; SAZ, Subantarctic Zone; PFZ: Polar Frontal Zone; SAF, Subantarctic Front; STF, Subtropical Front. Map created with Ocean Data View (Schlitzer, 2019).

from multiple Markov Chain Monte Carlo simulations of possible source contribution configurations, a range of possible source proportions consistent with the data can be developed.

One of the primary advantages of MixSIAR is that it also allows for users to input variability in source regions into the model (Parnell et al., 2010). Using means and standard deviations of source compositions MixSIAR uses a natural (Dirichelet; Forbes et al., 2011) probability distribution to develop potential model fits. As the Dirichelet-defined distribution is vague, the model is primarily driven by the data input from the user (Stock et al., 2018).

In dust provenance studies, contributions from different source regions may be highly variable, and the isotopic compositions of individual source regions may also cover wide ranges (Erhardt et al., 2021; Pichat et al., 2014; Struve et al., 2020; Trudgill et al., 2020). As such, an approach which allows for the incorporation of these uncertainties in the modeling of dust mixtures represents a considerable increase in accuracy when compared to typical (often simple binary mixing) source apportionment techniques. MixSIAR allows the user to consider more than two sources in each model. However, as the model assumes a contribution from each source (even if very small), increasing the number of sources decreases the certainty of model outputs. A final advantage of the MixSIAR model is that it also allows for the interpretation of datasets across a range of isotopic systems, with no limit to the number used. In this work we utilize this aspect and include Pb, Nd, and Sr isotope compositions in our model solutions. This yields further advantages in apportionment studies, as variability in source regions can sometimes only be distinguished via interpretation of multiple isotope systems.

3. Data Used in This Study

3.1. Source Data

We apply MixSIAR to two published multi-isotope (Nd, Sr, and Pb) dust composition datasets from the polar and subpolar South Pacific Ocean (Figure 1). The first dataset comprises core top samples of Holocene age (Wengler et al., 2019). We compare these to a dataset of isotopic compositions of dust deposited in the same region during the LGM (Struve et al., 2020).

Following the approach of Struve et al. (2020), we include Southern Hemisphere potential dust source areas (PSAs) in Australia, South America, and Africa. We consider Australia to encompass all dust sources from the

Australian continent and New Zealand. Antarctica is not considered as a major dust source during glacial intervals as the dust fluxes in the (sub)polar South Pacific (Lamy et al., 2014) are two orders of magnitude larger than dust fluxes at the Taylor Glacier located close to the most prominent Antarctic PSAs (Aarons et al., 2017). Similar differences in fluxes of terrigenic detritus are observed between Taylor Glacier and the (sub)polar South Pacific for the Holocene (Aarons et al., 2017; Wengler et al., 2019). We therefore follow the arguments of Struve et al. (2020) and include Antarctica primarily as a source of ice rafted debris (IRD) exported from the shelf seas to the polar South Pacific from the Ross Sea sector (Carlson et al., 2021; Hemming et al., 2007; Rackow et al., 2017). Notably, the IRD may contain particles that were previously deposited on the sea ice near potential dust sources in the Ross Sea area (Winton et al., 2014). The mean values of all PSA compositions and their single standard deviation (SD), which are the values used in the models, are listed in Table S1 in Supporting Information S1.

For those locations in the Holocene dataset that are located south of 68°S in the dataset (see Supporting Information S1), the lithogenic fluxes are significantly increased compared to the central South Pacific (Wengler et al., 2019). Therefore, we consider it likely that the composition of the dust fraction near the continental margin of West Antarctica is controlled by local input (Carlson et al., 2021). As such, we model these three Holocene samples separately, considering a range of isotopic source values from West Antarctica (Carlson et al., 2021), listed in Table S2 in Supporting Information S1. We note that this assumption is based on the fluxes of bulk lithogenic material at these sample locations (Wengler et al., 2019), whereas the <5 μm fraction may still contain significant amounts of dust from remote sources. However, the range of geochemical compositions of West Antarctic shelf and margin sediments (Carlson et al., 2021; Simões Pereira et al., 2018) overlaps with important dust source regions in Australia and South America. Hence, our model is unable to provide unequivocal quantification of local versus remote input sources of lithogenic <5 μm fraction particles at these three locations. We suggest that the available provenance and flux data could be complemented by grain size analysis to better distinguish between local versus remote sources of the lithogenic <5 μm fraction at these locations.

3.2. Model Optimization

Prior to any modeling, all sources were plotted on a series of two-dimensional cross sections of isotopic space. Using the mixing envelopes derived from this exercise, it is possible to ascertain which mixtures fall outside, and thus indicate a contributing source that has not been considered (Figure S1 in Supporting Information S1). When completed on our dataset, this exercise indicates two samples (one LGM and one Holocene; see Supporting Information) located very close to New Zealand that plot outside of mixing envelopes and cannot be modeled (see also below).

As recommended by previous work, we follow the approach of considering all possible sources in the initial model before combining model outputs a posteriori (Longman et al., 2018). Such an approach allows for the investigation of broad source changes (using grouped model outputs) and more specific shifts (using the raw outputs). We also model entire datasets initially (Holocene, LGM sediments, and Holocene samples from the West Antarctic margin; Figures 2 and 4a), before modeling each individual sample (Figures 3 and 4b,c). For the grouped outputs, we combine all potential sources into four primary source regions (a) Australia, (b) South America, (c) South Africa, and (d) Ross Sea (representative of IRD from Antarctica to the Southwest Pacific). All primary sources and groups used in this modeling, along with isotopic compositions and original references, are presented in Table S1 in Supporting Information S1. For the samples that are located close to Western Antarctica (Holocene samples south of 68°S), we present a separate model that only considers sources from Antarctica (Table S2 in Supporting Information S1), taken from Carlson et al. (2021). All model outputs are included in the Supporting Information S1.

To optimize the approach for the specific application of the model to dust provenance studies, we investigate the impact of changing specific model parameters on the model results using the sources listed in Table S1 in Supporting Information S1 with two examples; Holocene sample PS75/084-1 and LGM average value of core PS75/097-4.

Grouping model outputs a posteriori allows for both the consideration of all sources in the isotopic mixture and to improve the precision of modeled contributions (Longman et al., 2018). To illustrate this we compare the approach which considers all sources individually in the model to one in which all Australian sources are replaced

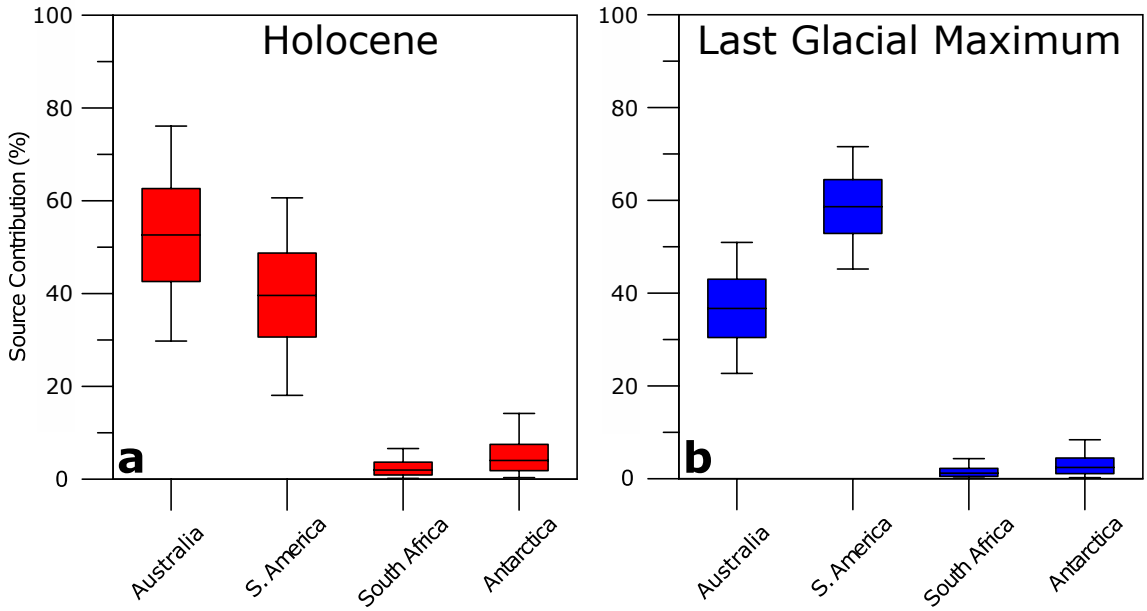

Figure 2. Grouped model outputs for the entire Holocene (panel a) and Last Glacial Maximum (panel b) datasets. Results are represented as box and whisker diagrams of all Monte Carlo simulations which satisfy the isotopic mass balance. Boxes are constructed using the interquartile range of the dataset and the median value, with whiskers denoting the 5th and 95th percentiles of the data.

by a single, integrated value, derived from the composition of dust deposited in the Tasman Sea (Borunda, 2019; Revel-Rolland et al., 2006; Struve et al., 2020). Comparison of these two approaches shows that a single integrated Australian source results in very low contributions from this source region to the Southwest Pacific for both the LGM and the Holocene. Instead, the model provides solutions for mixtures predominantly from sources in South America (Table S3 in Supporting Information S1), which appears unrealistic considering the proximity of the Southwest Pacific to Australia. This is an inherent feature of the model, related to the reduction of possible source regions in Australia/New Zealand, and results in an increased number of solutions calculated for the remaining source regions.

We also consider the effect of reducing the isotopic variability of the sources included in the model. Using a smaller standard deviation for the individual source regions should reduce overlap, and potentially tighten the range of model outputs. However, a reduction from 2SD to 1SD (Table S3 in Supporting Information S1) also reduces the ability of the model to capture the whole range of isotopic compositions in the source dataset. A test run with a sample from the Holocene and sample from the LGM shows that the 2SD solution is similar to the preferred model setup using 1SD (Table S3 in Supporting Information S1).

The combination of Sr, Nd, and Pb isotopes is a common approach in dust provenance studies (Grousset & Biscaye, 2005). Notably, Sr isotope compositions are sensitive to grain size and mineral sorting (Gili et al., 2017; Grousset & Biscaye, 2005; Struve et al., 2020), whereas the Nd and Pb isotope compositions are typically less affected by these processes (Garçon et al., 2014; Gili et al., 2017; Grousset & Biscaye, 2005). Therefore, we also test the dependence of the model output for the exclusion of Sr. Interestingly, the results of the exercise with and without the Sr isotope system display very similar model results (Table S3 in Supporting Information S1), but we exclude Sr from our preferred model approach to avoid potential grain size biases. Yet, we recommend its inclusion on a case-by-case basis after careful consideration of potential grain size effects.

A final option for this model is the implementation of different tracer concentrations in the terrestrial source material. MixSIAR allows users to input the elemental composition of sources to account for the higher sensitivity of a given sample mixture to contributions from highly concentrated sources (and vice versa for sources with lower concentrations; Phillips et al., 2014; Stock & Semmens, 2013). This is a valuable tool, and we compare the results of the modeling approach with and without this feature in Table S3 in Supporting Information S1, using concentration data, where available, as compiled by Struve et al. (2020) and for New Zealand from Koffman et al. (2021). The differences of Pb and Nd concentrations are small between the sources used in this work

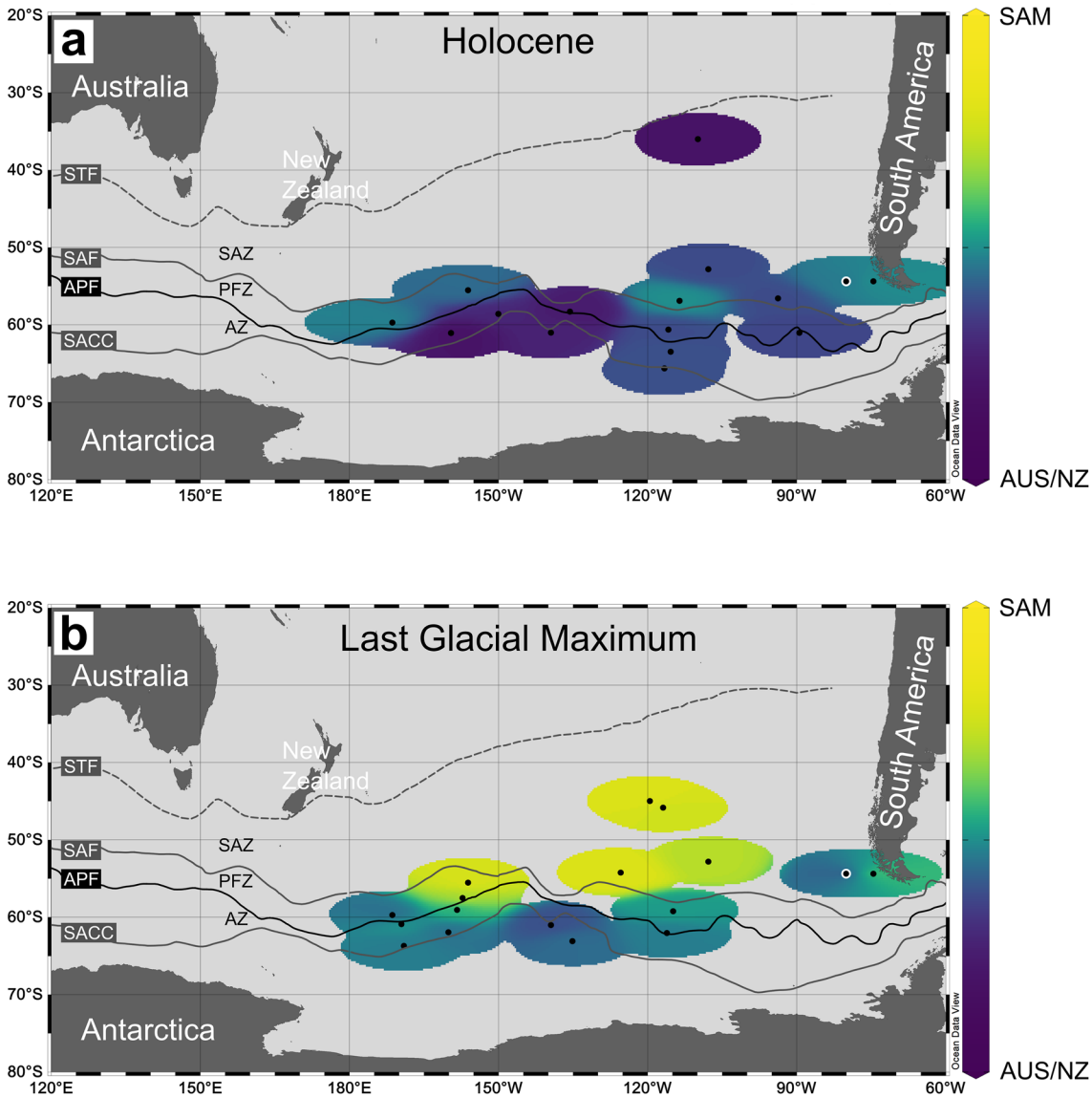

Figure 3. Proportions of dust input from Australia and New Zealand (AUS/NZ) and South America (SAM) for the Holocene (panel a) and the Last Glacial Maximum (panel b). In both panels black dots indicate the sampling locations, with the proportion of each source contributing to the mixture indicated by a color scale. Sample location PS75/034 indicated by white ring (see text for details). APF, Antarctic Polar Front; AZ, Antarctic Zone; PFZ, Polar Frontal Zone; SACC, Southern ACC Front; SAF, Subantarctic Front; SAZ, Subantarctic Zone; STF, Subtropical Front; Map created with Ocean Data View software (Schlitzer, 2019).

resulting in a negligible change in model outputs (Table S3 in Supporting Information S1). However, if large differences in element concentrations exist between individual sources (from ~1 order of magnitude variation), concentration data need to be implemented in order to generate accurate results. Due to the small variability in the element concentrations between the different Southern Hemisphere PSA and the incomplete nature of the elemental dataset (see Supporting Information in Struve et al., 2020), we use a model here that is not concentration dependent.

4. Results and Discussion

4.1. Model Limitations and Recommendations

It is crucial for the interpretation of the model outputs to consider also the limitations of the approach for dust provenance. The overlap of source compositions is a main limitation, as evident from the mixing envelopes

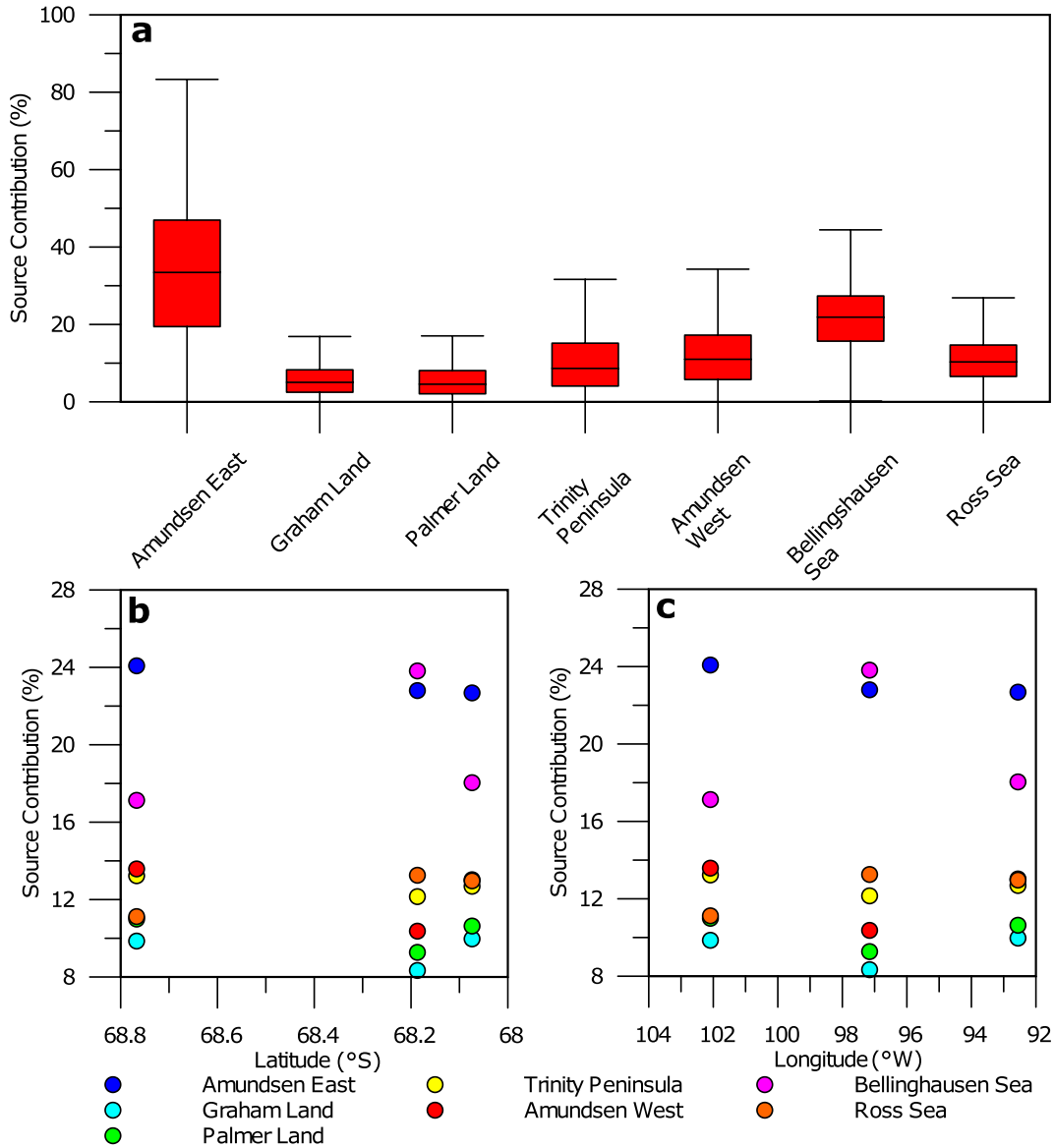

Figure 4. Grouped model output of samples south of 68°S (panel a), considering only West Antarctic sources. Results are represented as box and whisker diagrams of all Monte Carlo simulations which satisfy the isotopic mass balance. Boxes are constructed using the interquartile range of the dataset and the median value, with whiskers denoting the 5th and 95th percentiles of the data. Panels (b) and (c) display the average values of individual model outputs from each of these three samples, plotted against latitude and longitude, respectively.

(Figure S1 in Supporting Information S1). This overlap can complicate the identification of source contributions using MixSIAR. For example, New Zealand dust is very similar in composition to dust from the Lake Eyre basin (Table S1 in Supporting Information S1). The overlap can be reduced by using smaller SD values and/or the statistical removal of outliers (e.g., 2SD outlier tests). Furthermore, source overlap can be reduced by a more detailed assessment of the source regions, that is, breaking down or combining source regions prior to modeling. We applied this approach, for example, to the South American sources, which we subdivided into southern, central and northern sources in order to better constrain the range of dust compositions for the respective regions (Table S1 in Supporting Information S1). This subdivision is based on the geochemical composition of the source regions and is sensitive to latitudinal variations of the predominating westerly wind system (Struve et al., 2020). Without such subdivision, the continent would be considered a single source region resulting in a wide range of values and greater overlap with other sources (Table S1 in Supporting Information S1).

Once the initial models have been run, it may be possible to discern sources that do not contribute to the mixture. As MixSIAR always considers a contribution from all sources, no source will contribute 0%. However, if the model shows a specific source providing relatively low, but constant contributions to sample mixtures of different isotopic composition, it is justifiable to remove such sources from the model. Here, we considered source contributions of less than 5% mean contribution insignificant in the overall isotopic mixture. A re-run of the model without such insignificant sources provides then better constraints on the contributions from the remaining sources.

Our work also highlights some dust-specific and region-specific limitations. The first of these is the interpretation of sample compositions on the continental shelves, which can be affected by the input of local dust and rivers which may be poorly characterized, or not considered at all in the model. Furthermore, sample compositions on the continental shelves and slopes can be affected by mineral and/or grain size sorting during entrainment, transport and/or deposition of terrestrial particles (Garçon et al., 2014; Struve et al., 2020). For example, dust from the New Zealand continental shelf shows highly radiogenic Pb isotope compositions, which fall outside of the mixing envelope (see Supporting Information). Recent work presented Pb isotope compositions for a location at the east coast from New Zealand's South Island (Erhardt et al., 2021) similar to the signal recovered from shelf and margin sediments offshore (Struve et al., 2020; Wengler et al., 2019), but different to any other terrestrial signal in this source region (Koffman et al., 2021). A highly radiogenic Pb isotope signal has been identified for intraplate volcanic rocks in New Zealand (Hoernle et al., 2006), but their Nd and Sr isotope compositions are inconsistent with available terrestrial (Koffman et al., 2021) and shallow-marine fine fraction data in the area (Struve et al., 2020; Wengler et al., 2019). Therefore, it is likely that sorting processes during sediment transport have led to an accumulation of minerals which contain greater proportions of radiogenic Pb (Garçon et al., 2014; Struve et al., 2020). Another example of this feature may be seen in samples from the Patagonian shelf where our models reconstruct a fairly equal Australian and South American contribution (DataSet S1 in Supporting Information S2; Figure 3), although local sources likely contribute the majority of dust fraction particles. We therefore recommend considering the depositional setting at specific locations and the inclusion of complementary methods of dust reconstruction such as lithogenic input fluxes and dust particle size analysis in the data interpretation.

4.2. Large-Scale Changes Between Holocene and LGM Dust Provenance

The modeling approach utilized here can clearly identify large-scale trends in contributions from individual sources to the dust deposition in the South Pacific. Using the sources in Table S1 in Supporting Information S1, the contribution from both Antarctica and South Africa is low across all models (Figure 2). For South Africa, this is in line with previous interpretations of isotopic mixtures for Holocene and LGM dust in the study area (Struve et al., 2020; Trudgill et al., 2020; Wengler et al., 2019), and model reconstructions of dust sources during the LGM (Albani et al., 2012). The lack of a considerable component from Ross Sea sources also supports previous work suggesting modest contributions of IRD to the dust fraction of sediments in the polar Southwest Pacific for both the Holocene configuration (Wengler et al., 2019) and the LGM (Struve et al., 2020).

For the Holocene samples close to the West Antarctic shelves (Figure 1), we consider local sources (Table S2 in Supporting Information S1; Carlson et al., 2021), because the lithogenic fluxes at these locations are clearly elevated compared to the central South Pacific typically regarded as dust-dominated (Lamy et al., 2014; Wengler et al., 2019). The main contributor of dust fraction material is the nearby Amundsen East area (following the nomenclature of Carlson et al., 2021; Figure 4) substantiating the idea of a direct input of local lithogenic material from the shelves at these locations (Wengler et al., 2019). However, this modeling scenario is based on the assumption that the elevated fluxes of (bulk) lithogenic material observed at these locations (Wengler et al., 2019) dominate also the deposition of <5 μm fraction particles. We note that this may not be the case, but due to the wide range of isotopic compositions of sediments on the West Antarctic shelves, it is not possible to unequivocally distinguish between the contribution from local sources and the input from remote terrestrial sources.

The dust input at the remote open ocean locations is dominated by sources in Australia and South America with specific changes and trends in both, the Holocene and the LGM results. This is demonstrated by the shift in average South American dust contribution between all Holocene remote open ocean samples (mean 30%, $n = 18$) and LGM samples (mean 54%, $n = 15$), and the increase in Australian contribution from the LGM (mean 38%) to the Holocene (mean 56%; Figure 2). One exception is open ocean sample location PS75/034 in the Southeast Pacific showing a relatively invariable composition for both time intervals which is distinct from the remaining open

Table 1
Correlation Coefficients (Pearson's r) Between Individual Model Outputs and Longitude or Latitude, for Grouped Continental Sources

Holocene	Latitude	*p*-value	Longitude	*p*-value	*n*
Australia	0.26	0.30	−0.23	0.35	18
South America	−0.31	0.21	0.10	0.70	18
LGM	**Latitude**	***p*-value**	**Longitude**	***p*-value**	***n***
Australia	−0.84	*<0.01*	−0.38	0.16	15
South America	0.84	*<0.01*	0.38	0.16	15

Note. Statistically significant at the fifth percentile (p-value <0.05) regressions are highlighted in italics.

ocean dataset (DataSet S1 and S2 in Supporting Information S2, Figures 3a and 3b). Like the locations close to the continental margins (see above), location PS75/034 is not included in the statistical analysis of the large-scale trends in dust provenance discussed below.

The general picture of Holocene dust provenance is further supported by the model solution for the different grain size fractions (Figure S2 in Supporting Information S1). This is interesting considering that it has been hypothesized that the different grain size fractions in Holocene samples from the South Pacific may be influenced to different degrees by anthropogenic particles (Struve et al., 2020). Overall, the model output supports previous work which has indicated a shift toward increased dust input from South American sources during the LGM, as a result of enhanced South American dust entrainment and transport at this time (Struve et al., 2020). In particular, our model ascertains maximum contributions of up to ~75% of dust from South American sources, further substantiating previous conclusions based on binary mixing calculations (Struve et al., 2020).

4.3. Spatial Variations of the Dust Fraction Composition in the South Pacific

The model results resolve spatial trends in both, the Holocene and the LGM. In the Holocene dataset, we observe weak correlations between longitude and mean contributions from both Australia and South America (Table 1, Figures 3 and 5). Our data show a tendency toward an increased contribution of dust from Australia in the western South Pacific during the Holocene, consistent with air mass and dust models (Li et al., 2008; Neff & Bertler, 2015), but also the eastward decrease of the Australian dust contribution relative to South American dust. As the dust plumes travel predominantly eastwards at these latitudes (De Deckker et al., 2010; Li et al., 2008; Neff & Bertler, 2015; Wengler et al., 2019), this would suggest that Australian dust fallout has a shorter residence time over the South Pacific compared to dust reaching the area from South America, explaining the significant influence of local sources on lithogenic input near New Zealand (Trudgill et al., 2020; Wengler et al., 2019; Wu et al., 2021). Our results also show that the absolute contributions and spatial trends of dust from individual sources in Australia are distinct across the study area (Figure 7a). This may be related to different trends of regional environmental change in important Australian dust source areas during the Holocene (e.g., Fitzsimmons et al., 2013; Marx et al., 2009), probably contributing to the relatively high variability of the dust fraction provenance signal in the Holocene sediments (reflecting also different age intervals due to their different depositional settings) in the Southwest Pacific (Wengler et al., 2019; Figure 3).

Previous research has suggested that the Lake Eyre basin is the primary contributor of dust from Australian sources to the Holocene South Pacific (De Deckker et al., 2010; McGowan & Clark, 2008; Revel-Rolland et al., 2006; Wengler et al., 2019). Here, we revisit this suggestion by using the raw outputs (prior to a posteriori grouping) from the Holocene models (Figures 7a and 7c). For this exercise, we calculate the contribution of each Australian source as a proportion of the total contribution from Australia, rather than as a proportion of the total dust mixture (see caption of Figure 6 for more details). This approach shows that the Lake Eyre basin contributes an average of 33% to the total amount of Australian dust deposited in the South Pacific during the Holocene (i.e., 17% of all dust). New Zealand is the second most considerable source from this region (mean 26%), with the Darling basin contributing on average 18% of the Australian component (Figure 6a). Sources from New Zealand show geochemical similarity with important PSA in Australia, limiting the significance of both, simple mass balance calculations (Struve et al., 2020; Wengler et al., 2019) and Bayesian modeling approaches (this work).

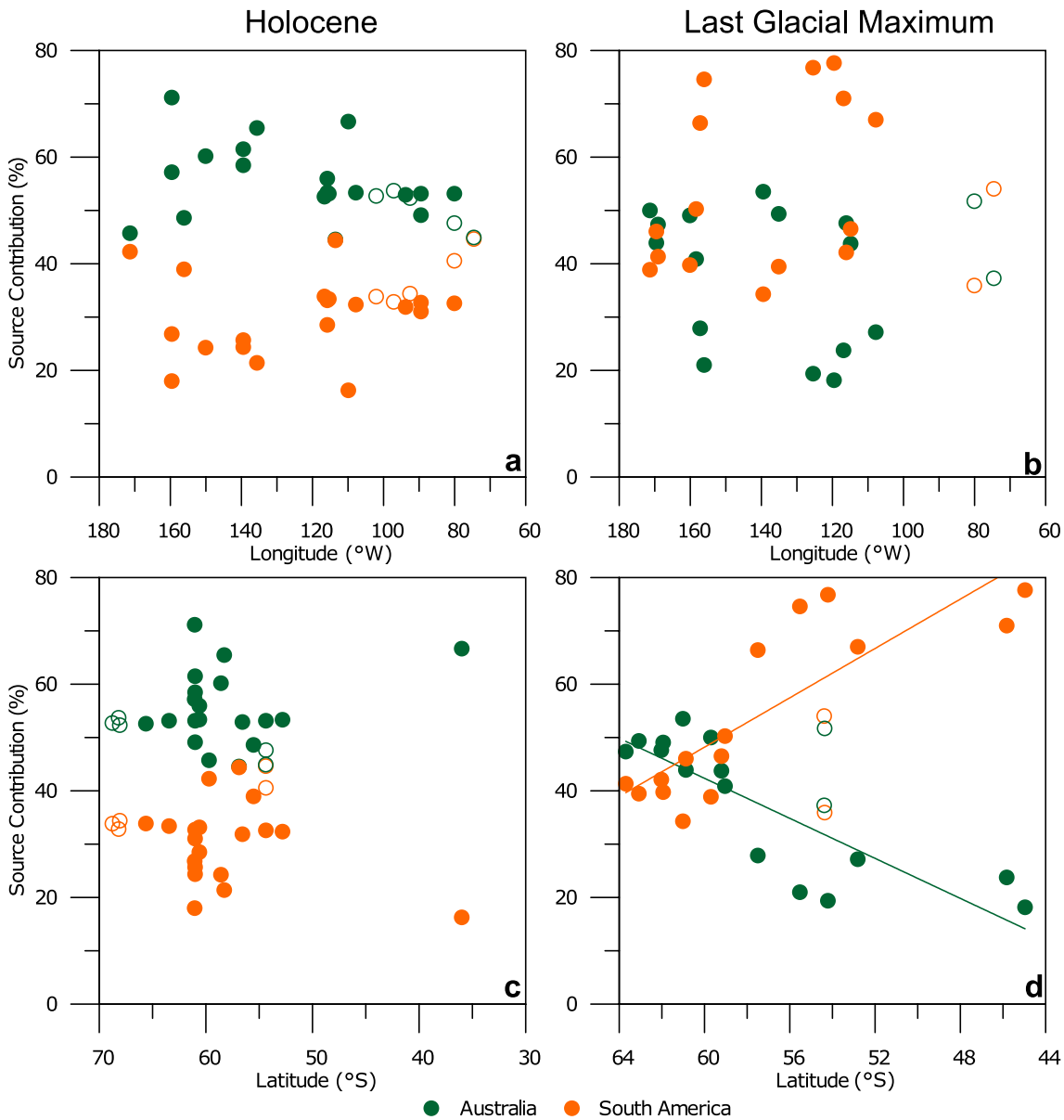

Figure 5. Model outputs representing the contribution of South American (orange circles) and Australian (green circles) sources to individual sample mixtures, plotted against longitude and latitude. Unfilled circles indicate those which are not considered open ocean, and so are not included in statistical analysis (see Methods). Panels a and b are the contributions from the two sources plotted against longitude for the Holocene and Last Glacial Maximum (LGM) configuration, respectively. Panels c and d are source contributions plotted against latitude, again for the Holocene and LGM configuration, respectively. In each case, circles indicated the mean output of each model. Linear regression fits are indicated by solid lines in respective colors if they are considered statistically significant at the 0.05 level (i.e., a p-value <0.05; see Table 1). Details on these regressions can be found in Table 1.

Yet, our findings largely support data based and modeled evidence suggesting that the Lake Eyre basin is the most active source of dust on the Australian continent, with the Darling basin a secondary component of the mixture (De Deckker, 2019; De Deckker et al., 2010; McGowan & Clark, 2008; McTainsh, 1989; Prospero, 2002; Wengler et al., 2019). Investigation of the outputs from individual models can provide additional insight into the trends of Australian dust contributions in the Holocene samples (Table 2, Figures 6a, 7a, and 7c). No significant correlations are observed between changes in Australian source contributions and latitude in these Holocene samples (Figure 7c). There is a positive correlation between the contribution from Lake Eyre and longitude for the Holocene samples (r = 0.48, p-value <0.05, n = 18), indicating that a higher proportion of dust entrained from this basin is transported further east into the South Pacific than other Australian sources via the "Southeast

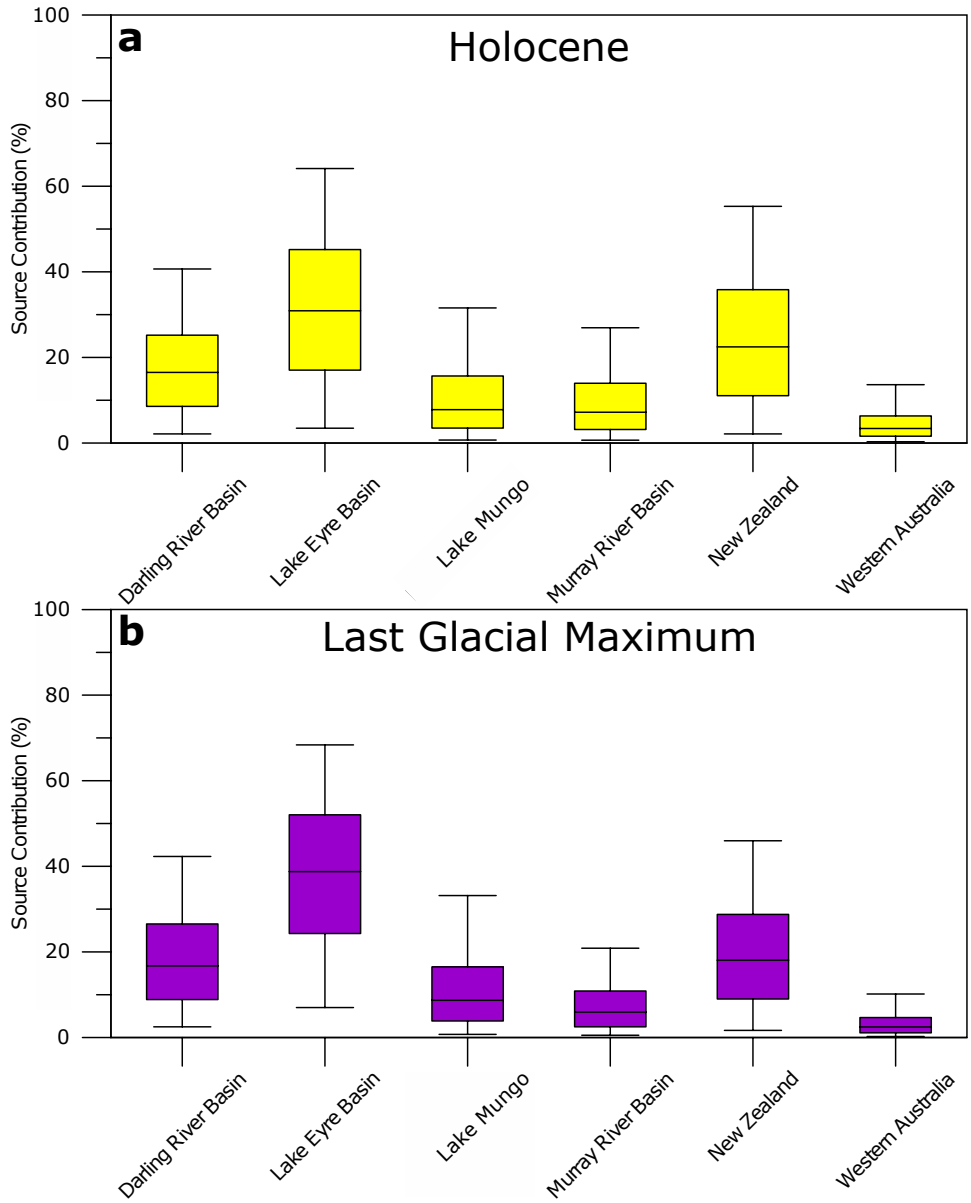

Figure 6. Grouped model output of Australian sources for the Holocene (panel a) and LGM (panel b) datasets. Results are represented as box and whisker diagrams of all Monte Carlo simulations which satisfy the isotopic mass balance. Boxes are constructed using the interquartile range of the dataset and the median value, with whiskers denoting the 5th and 95th percentiles of the data. Note that these results are based on all model solutions for the individual source regions, that is, different to the average values of individual model outputs for the South Pacific samples shown in Figure 7.

dust transport corridor" (McGowan & Clark, 2008), whereas the total contribution of Australian dust decreases eastward (Figure 5a). Contributions of dust from other sub-continental scale sources show also tendencies for zonal changes, but the regressions are not statistically significant at the 0.05 level (Table 2). Notably, the relative proportion of dust from western Australia seems to be lower at the eastern compared to the western sites, as illustrated by a negative correlation ($r = -0.45$, p-value $= 0.06$, $n = 18$; see Table 2). However, the modeled Western Australian component in these Holocene samples from the central polar South Pacific may also be explained by a possible contribution from anthropogenic particulates and/or specific IRD sources to these samples having an overall extremely low trace metal content (see Struve et al., 2020; Wengler et al., 2019; Supporting Information). Since we are unable to fully characterize the composition of possible anthropogenic and/or rare IRD particles in these samples we suggest careful interpretation of the results for these specific samples.

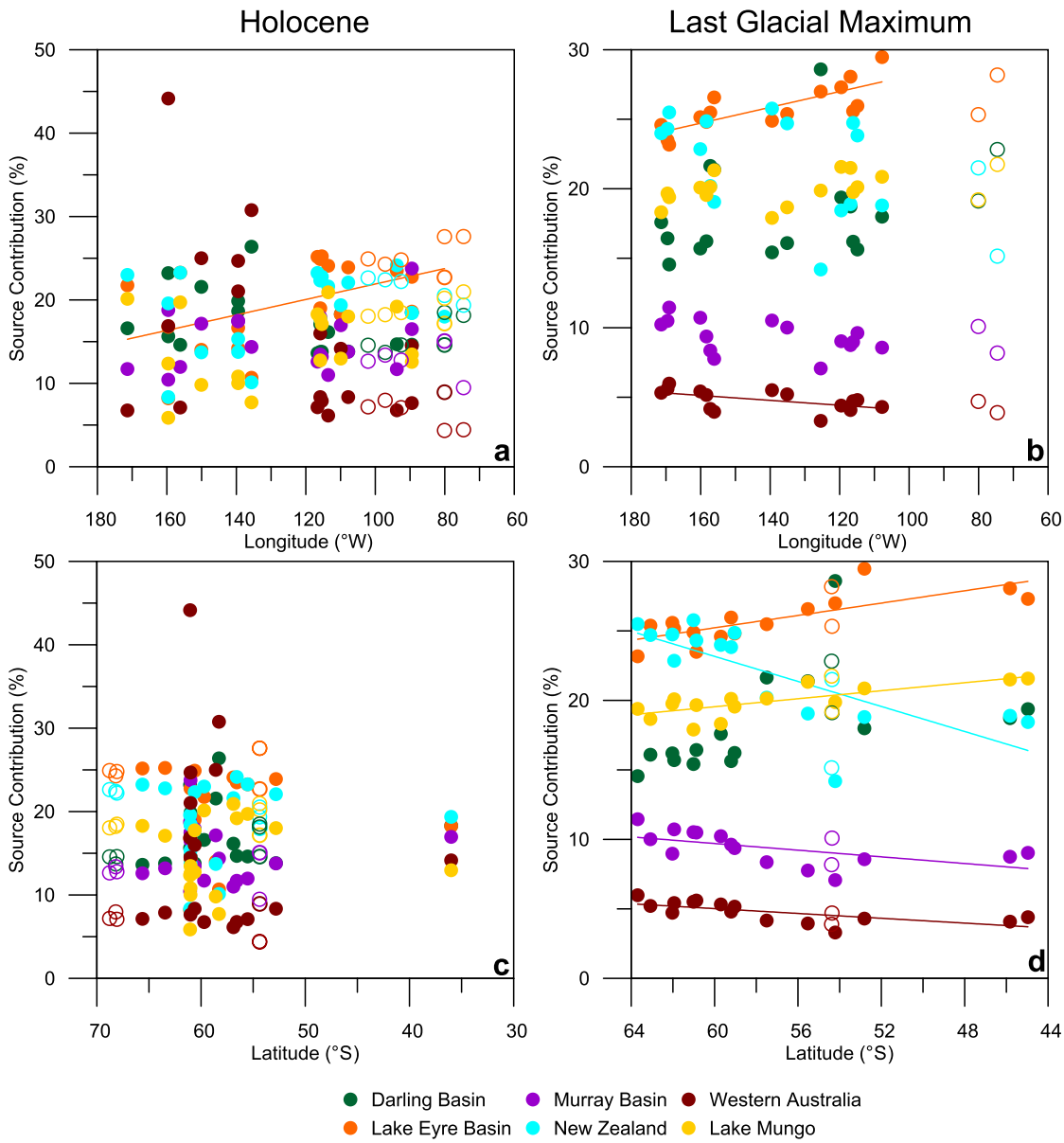

Figure 7. Contributions from individual Australian sources to the total amount of dust exported from the Australian region to the South Pacific (see text for details). Unfilled circles indicate those which are not considered remote open ocean, and so are not included in statistical analysis (see Methods). Panels a and b display the contribution of each individual source to the mixture plotted against longitude, for the Holocene and LGM configuration, respectively. Panels c and d are source contributions plotted against latitude, again for the Holocene and LGM configuration, respectively. Linear regressions are indicated if they are considered statistically significant at the 0.05 level (i.e., a p-value <0.05; see Table 2 for details). Note that excluding LGM10 from the results shown in panel (d) would yield a p-value of 0.02 for the Darling Basin LGM data versus latitude (see DataSet S2 in Supporting Information S2). Details on these regressions are listed in Table 2. Note also different y-axis scales in (a) and (c) versus (b) and (d).

For the LGM, our modeling results show that Australian contributions were broadly similar, but accounted for a smaller proportion of the isotopic mixture. Lake Eyre remains the primary Australian source (mean 39%), with New Zealand (mean 20%) and the Darling Basin (mean 18%) being again the other main source regions (Figure 6b). The similarity in contributions between the two periods suggests that the same general source regions were active in Australia/New Zealand during the LGM and the Holocene, a finding supported by previous studies which have indicated the importance of Lake Eyre as a source for LGM dust in the South Pacific (Molina-Kescher et al., 2016; Revel-Rolland et al., 2006; Struve et al., 2020). The latitudinal changes dominate the spatial trends in the LGM open ocean dataset with an overall higher contribution from South American sources and an increase toward the north (Figure 3), reflected in correlations between latitude and the contribution from South American

Table 2
Correlation Coefficients (Pearson's r) Between Individual Model Outputs and Longitude or Latitude, for Individual Australian and South American Sources

Holocene	Latitude	*p*-value	Longitude	*p*-value	*n*
Darling Basin	0.06	0.80	−0.37	0.13	18
Lake Eyre Basin	−0.02	0.95	0.48	*0.05*	18
Lake Mungo	0.05	0.84	0.23	0.34	18
Murray Basin	0.02	0.95	0.24	0.35	18
New Zealand	0.09	0.73	0.33	0.18	18
Western Australia	−0.08	0.74	−0.45	0.06	18
S. America 20–24°S	−0.05	0.84	−0.11	0.66	18
S. America 24–32°S (selected)	−0.06	0.80	0.05	0.85	18
S. America >32°S	0.10	0.69	−0.02	0.93	18
LGM	**Latitude**	***p*-value**	**Longitude**	***p*-value**	***n***
Darling Basin	0.48	0.07	0.18	0.52	15
Lake Eyre Basin	0.77	*<0.01*	0.78	*<0.01*	15
Lake Mungo	0.76	*<0.01*	0.41	0.13	15
Murray Basin	−0.58	*0.02*	−0.48	0.07	15
New Zealand	−0.76	*<0.01*	−0.41	0.13	15
Western Australia	−0.68	*<0.01*	−0.54	*0.04*	15
S. America 20–24°S	−0.80	*<0.01*	−0.42	0.12	15
S. America 24–32°S (selected)	0.80	*<0.01*	0.42	0.12	15
S. America >32°S	−0.79	*<0.01*	−0.42	0.12	15

Note. Statistically significant at the fifth percentile (*p*-value <0.05) regressions are highlighted in italics.

sources ($r = 0.84$, p-value <0.01, $n = 15$) and Australian sources, respectively (Figure 5). This tallies well with previous work, which has indicated that during the LGM intensified westerlies brought greater amounts of South American dust into the South Pacific in general and to the Subantarctic Zone in particular (Struve et al., 2020). Furthermore, our model results reveal strong positive correlations between latitude and individual Australian source regions (i.e., greater contribution to northern sites) for the Lake Eyre, Lake Mungo, and Darling basins (Table 2; Figure 7d). This suggests greater transport of dust from these PSA to the subpolar South Pacific during the LGM relative to other Australian sources (note that the relative contribution of Australian sources to the total dust deposition was lower during the LGM). In contrast, negative correlations between latitude and dust from New Zealand, Western Australia and the Murray Basin indicate reduced long-distance transport from these sources to the subpolar South Pacific (Table 2; Figures 6b and 7d). The LGM dust transport from all these source areas to the mid-latitude South Pacific is controlled by the Southern Hemisphere Westerly Winds (SWW; Lamy et al., 2014; Struve et al., 2020, van der Does et al., 2021). As such, the distinct latitudinal trends in the contribution of individual PSA to the total Australian dust export are probably the result of specific (seasonal) changes in the source areas (moisture conditions, vegetation cover, sediment availability etc.; De Deckker et al., 2020; Ginoux et al., 2012; McTainsh, 1989; Prospero, 2002), their interaction with local winds and the predominating SWW system (De Deckker et al., 2010; Marx et al., 2009; McGowan et al., 2005; McTainsh, 1989) and the conditions of deposition in the study area (e.g., sea-ice cover, particle settling; Struve et al., 2020).

Our LGM model output also reveals a pronounced longitudinal variation of Australian source contributions, expressed in a positive correlation between the Lake Eyre basin and longitude ($r = 0.78$, p-value =<0.01, $n = 15$), again suggesting a greater contribution from this source to the eastern sites compared to other Australian sources (Figures 7b and Table 2). This implies particularly high levels of long-distance transport of dust from this area of Australia during the LGM, whereas the Murray Basin in Southeast Australia and New Zealand show negative correlations and thus a reduced range of Australian dust exported from these PSA (Figure 7b). We completed a similar exercise for South American sources (Figure 8). Using this approach, a lack of correlation between

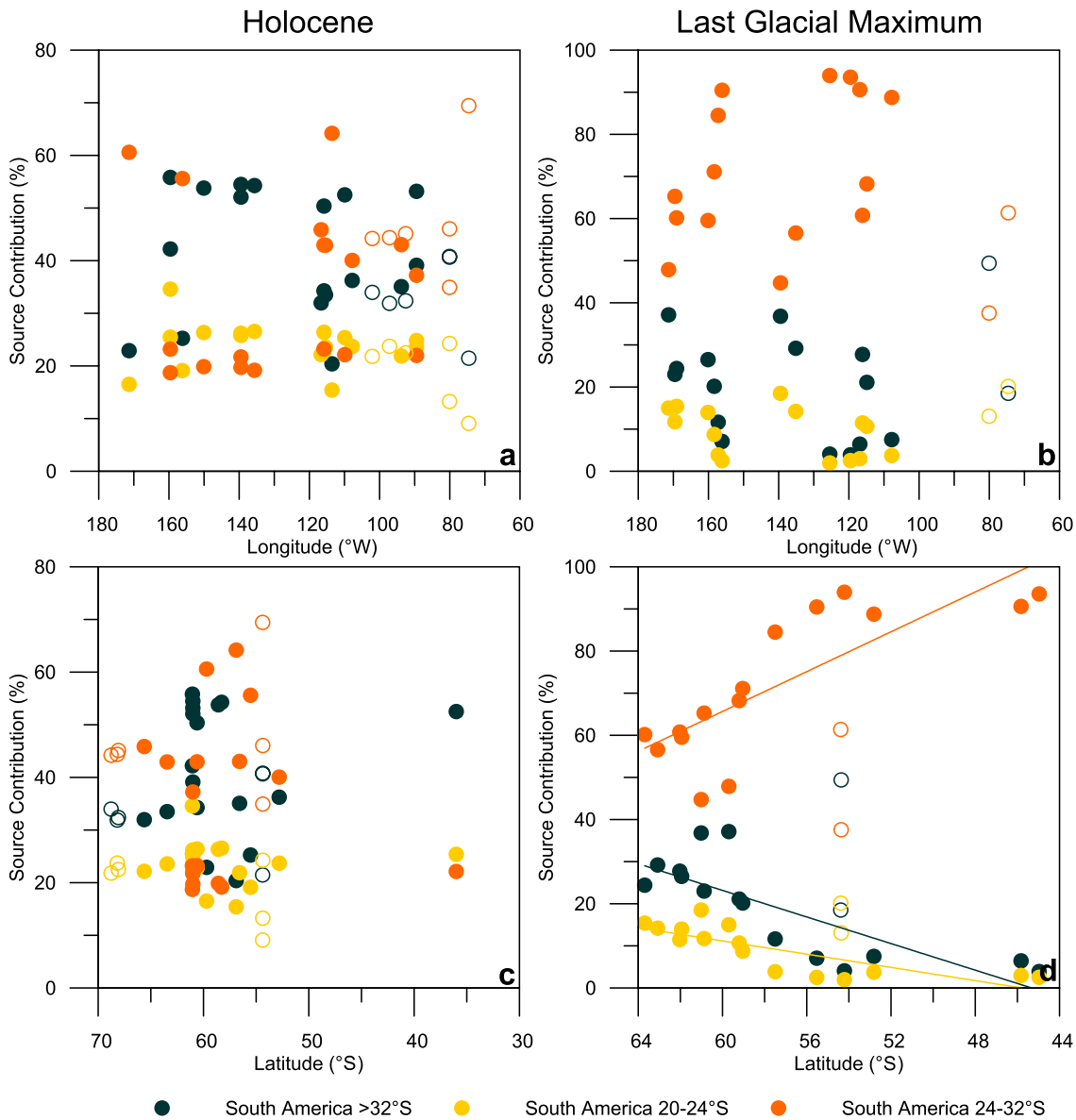

Figure 8. Contributions from individual South American sources to the total amount of dust exported from South America to the South Pacific (see text for details). Panels (a) and (b) display the contribution of each individual source to the mixture plotted against longitude, for the Holocene and LGM configuration, respectively. Panels (c) and (d) are source contributions plotted against latitude, again for the Holocene and LGM configuration, respectively. Unfilled circles represent samples not used in statistical analyses as described in caption of Figure 7. Linear regressions are indicated if they are considered statistically significant at the 0.05 level (i.e., a p-value <0.05; see Table 2 for details). Note different y-axis scales in (a) (c) versus (b) (d).

longitude or latitude during the Holocene can be observed, with all three PSAs contributing variable amounts of dust to the mixtures. In contrast, it is clear that central South American (24–32°S) dust predominates during the LGM, comprising up to ~90% of all South American dust preserved in some cores (Figures 8b and 8d). This finding supports the assertions of Struve et al. (2020), who concluded that the radiogenic Pb isotope signal observed in South Pacific dust during the LGM was derived from a central South American source (which is geochemically distinct from the regions to the south and north; Gili et al., 2017) and delivered to the study area by strong westerly winds. Active dust emissions from this source region have been proposed to contribute to the dust deposition in East Antarctic ice cores during glacial times (Gili et al., 2017) and satellite observations reveal that dust plumes are moved around the globe by high altitude westerly winds (Uno et al., 2009). The similar spatial trends of far-travelled dust from Central South American and Central/East Australian sources (Figures 7 and 8; Table 2) further support the idea that the westerly wind circulation plays an important role in the distribution of

dust from both continents across the South Pacific (Struve et al., 2020). At the same time, the dust delivered to the Southeast Pacific during the LGM was coarser than dust reaching the area during the Holocene (van der Does et al., 2021). Therefore, the high proportion of South American dust in the subpolar Southeast Pacific suggests that the delivery of larger far-travelled dust particles during the LGM was related to longer atmospheric residence times of the dust particles and higher wind speeds of the circumpolar westerly wind system rather than an increased contribution from a single proximal source alone.

4.4. Further Work and Outlook

Our work has demonstrated the applicability of Bayesian mixing models to multi-isotope provenance studies of dust deposition and we propose to apply this approach more widely to (dust) provenance studies. The application of such model approach can provide improved estimates of source contributions, and thus supporting interpretation of datasets, for all spatial and temporal scales.

The construction of the model also allows for the inclusion of more variables, each of which may help further constrain source provenance. For dust related studies, one such variable is the rare earth element (REE) content. REEs can be enriched or depleted as a result of changing mineralogy (Ferrat et al., 2011; Yang et al., 2007), and may provide an additional tracer of dust provenance (Gili et al., 2017; Struve et al., 2020). In addition, other provenance tracers such as Sr, Hf, or Th-He isotopes (Blakowski et al., 2016; Grousset & Biscaye, 2005; McGee et al., 2016) can be included to help distinguishing between sources which otherwise have very similar Pb and Nd isotope compositions. Finally, we anticipate to expand the use of non-traditional stable isotope analyses as source tracers in the future (Schleicher et al., 2020), especially in studies which consider anthropogenic sources (Souto-Oliveira et al., 2018). To this end, the isotopic systems of elements such as copper, zinc and iron could potentially yield useful source information and may easily be included in future MixSIAR modeling.

In this work, we have only considered the contribution of each source to the mixture, a method which does not allow for the interpretation of absolute levels of dust to be interpreted. For example, although our work shows greater Australian dust input to the Holocene South Pacific than during the LGM, it is not possible to know exactly how much dust this represents. This information is however provided by complementary dust flux data showing a substantial increase in dust fluxes in the subpolar South Pacific during the LGM (Lamy et al., 2014; Shoenfelt et al., 2018). For example, lithogenic flux estimates are available for both the Holocene (Wengler et al., 2019) and LGM (Lamy et al., 2014) at location PS75/076 (Figure 1). Using the Holocene provenance model output for this core (Figure 3), we estimate the absolute flux of Australian dust to be 0.5 g/m^2/year, with 0.28 g/m^2/year from South America. For the LGM, the absolute Australian contribution remains similar, at 0.68 g/m^2/year, but the South American component is much greater, at 0.97 g/m^2/year. Consequently, the output of our models can be combined with lithogenic flux calculations, to convert from proportional data into absolute depositional values at locations where lithogenic fluxes reflect atmospheric dust input.

5. Conclusions

Here, we present the results of the utilization of a Bayesian mixing model to apportion source contributions to dust mixtures, using their Pb and Nd isotope compositions in the South Pacific. Our work clearly shows the applicability of this approach and that the model results are dominated by Pb and Nd isotope compositions, whereas the moderate variation of metal concentrations in the source material as well as the Sr isotope composition have only very modest influence on the overall results. Testing different model configurations reveals that grouping multiple small source areas to a single continental scale dust source can lead to biased results in comparison to using multiple smaller subcontinental scale sources and grouping the individual contributions a posteriori. Our model output supports previous work by indicating a high proportion of South American dust deposition in the South Pacific during the LGM, but also a contribution from this source to the Holocene dust fraction. During both time periods the remaining portion is supplied predominantly by Australian sources.

In addition, our results reveal spatial trends in the data. For the Holocene configuration, the contribution of Australian dust tends to decrease eastward relative to the contribution from South American sources, thus indicating a reduced atmospheric residence time of Australian dust over the South Pacific. In contrast, the LGM dataset is dominated by strong latitudinal gradients with a contribution of up to 75% of the total dust deposition in the subpolar South Pacific being sourced from South America. Our work has also investigated the contribution of

sub-continental scale source areas to the total amount of dust exported from Australia and South America, respectively. We identified the Lake Eyre basin as the most important contributor of dust from Australia during both the LGM and the Holocene, with an eastward increasing proportion of dust from the Lake Eyre basin in the total amount of Australian dust delivered to the southern South Pacific. However, the distribution patterns of dust from the individual sub-continental scale source areas, both in Australia and South America, show predominantly latitudinal trends during the LGM with the most prominent of these trends being the northward increase of dust input from Central South America. The relatively coarse dust fraction sediments in the subpolar Southeast Pacific were consequently delivered from both South American and Australian sources during the LGM, which requires increased atmospheric residence times and an accelerated glacial westerly wind regime facilitating the circumpolar atmospheric transport of coarser-than-Holocene dust.

Data Availability Statement

All data produced in this study are available in the Supporting Information S1 file and under doi: https://doi.org/10.6084/m9.figshare.17074811. All geochemical data used in this modeling study are available in Wengler et al. (2019), Struve et al. (2020) and Carlson et al. (2021). The MixSIAR model is available in Stock and Semmens (2013) and Stock et al. (2018).

Acknowledgments
We acknowledge financial support from the University of Oldenburg and the DFG. Open access funding enabled and organized by Projekt DEAL.

References

Aarons, S. M., Aciego, S. M., Arendt, C. A., Blakowski, M. A., Steigmeyer, A., Gabrielli, P., et al. (2017). Dust composition changes from Taylor Glacier (East Antarctica) during the last glacial-interglacial transition: A multi-proxy approach. *Quaternary Science Reviews*, *162*, 60–71. https://doi.org/10.1016/j.quascirev.2017.03.011

Aciego, S. M., Riebe, C. S., Hart, S. C., Blakowski, M. A., Carey, C. J., Aarons, S. M., et al. (2017). Dust outpaces bedrock in nutrient supply to montane forest ecosystems. *Nature Communications*, *8*, 1–10, 14800. https://doi.org/10.1038/ncomms14800

Albani, S., Mahowald, N. M., Delmonte, B., Maggi, V., & Winckler, G. (2012). Comparing modeled and observed changes in mineral dust transport and deposition to Antarctica between the Last Glacial Maximum and current climates. *Climate Dynamics*, *38*, 1731–1755. https://doi.org/10.1007/s00382-011-1139-5

Albani, S., Mahowald, N. M., Murphy, L. N., Raiswell, R., Moore, J. K., Anderson, R. F., et al. (2016). Paleodust variability since the Last Glacial Maximum and implications for iron inputs to the ocean. *Geophysical Research Letters*, *43*, 3944–3954. https://doi.org/10.1002/2016GL067911

Blain, S., Quéguiner, B., Armand, L., Belviso, S., Bombled, B., Bopp, L., et al. (2007). Effect of natural iron fertilization on carbon sequestration in the Southern Ocean. *Nature*, *446*, 1070–1074. https://doi.org/10.1038/nature05700

Blake, W. H., Boeckx, P., Stock, B. C., Smith, H. G., Bodé, S., Upadhayay, H. R., et al. (2018). A deconvolutional Bayesian mixing model approach for river basin sediment source apportionment. *Scientific Reports*, *8*, 1–12. https://doi.org/10.1038/s41598-018-30905-9

Blakowski, M. A., Aciego, S. M., Delmonte, B., Baroni, C., Salvatore, M. C., & Sims, K. W. W. (2016). A Sr-Nd-Hf isotope characterization of dust source areas in Victoria Land and the McMurdo Sound sector of Antarctica. *Quaternary Science Reviews*, *141*, 26–37. https://doi.org/10.1016/j.quascirev.2016.03.023

Borunda, A. (2019). *Tracing dust in the Southern Hemisphere over the last glacial cycle (Doctoral dissertation)*. New York, NY: Columbia University. https://doi.org/10.7916/d8-rmak-548

Boyd, P. W., Mackie, D. S., & Hunter, K. A. (2010). Aerosol iron deposition to the surface ocean - modes of iron supply and biological responses. *Marine Chemistry*, *120*, 128–143. https://doi.org/10.1016/j.marchem.2009.01.008

Browning, T. J., Achterberg, E. P., Engel, A., & Mawji, E. (2021). Manganese co-limitation of phytoplankton growth and major nutrient drawdown in the Southern Ocean. *Nature Communications*, *12*, 884. https://doi.org/10.1038/s41467-021-21122-6

Carlson, A. E., Beard, B. L., Hatfield, R. G., & Laffin, M. (2021). Absence of West Antarctic-sourced silt at ODP site 1096 in the Bellingshausen sea during the last interglaciation: Support for West Antarctic ice-sheet deglaciation. *Quaternary Science Reviews*, *261*, 106939. https://doi.org/10.1016/j.quascirev.2021.106939

De Deckker, P. (2019). An evaluation of Australia as a major source of dust. *Earth-Science Reviews*, *194*, 536–567. https://doi.org/10.1016/j.earscirev.2019.01.008

De Deckker, P., Moros, M., Perner, K., Blanz, T., Wacker, L., Schneider, R., et al. (2020). Climatic evolution in the Australian region over the last 94 ka - Spanning human occupancy -, and unveiling the Last Glacial Maximum. *Quaternary Science Reviews*, *249*, 106593. https://doi.org/10.1016/j.quascirev.2020.106593

De Deckker, P., Norman, M., Goodwin, I. D., Wain, A., & Gingele, F. X. (2010). Lead isotopic evidence for an Australian source of aeolian dust to Antarctica at times over the last 170,000 years. *Palaeogeography, Palaeoclimatology, Palaeoecology*, *285*, 205–223. https://doi.org/10.1016/j.palaeo.2009.11.013

Delmonte, B., Paleari, C. I., Andò, S., Garzanti, E., Andersson, P. S., Petit, J. R., et al. (2017). Causes of dust size variability in central east Antarctica (Dome B): Atmospheric transport from expanded south American sources during marine isotope stage 2. *Quaternary Science Reviews*, *168*, 55–68. https://doi.org/10.1016/j.quascirev.2017.05.009

Erhardt, A. M., Douglas, G., Jacobson, A. D., Wimpenny, J., Yin, Q. Z., & Paytan, A. (2021). Assessing sedimentary detrital Pb isotopes as a dust tracer in the Pacific Ocean. *Paleoceanography and Paleoclimatology*, *36*, e2020PA004144. https://doi.org/10.1029/2020PA004144

Ferrat, M., Weiss, D. J., Strekopytov, S., Dong, S., Chen, H., Najorka, J., et al. (2011). Improved provenance tracing of Asian dust sources using rare earth elements and selected trace elements for palaeomonsoon studies on the eastern Tibetan Plateau. *Geochimica et Cosmochimica Acta*, *75*, 6374–6399. https://doi.org/10.1016/j.gca.2011.08.025

Fitzsimmons, K. E., Cohen, T. J., Hesse, P. P., Jansen, J., Nanson, G. C., May, J.-H., et al. (2013). Late Quaternary palaeoenvironmental change in the Australian drylands. *Quaternary Science Reviews*, *74*, 78–96. https://doi.org/10.1016/j.quascirev.2012.09.007

Forbes, C., Evans, M., Hastings, N., & Peacock, B. (2011). *Statistical distributions* (4th Ed.). Wiley.

Garçon, M., Chauvel, C., France-Lanord, C., Limonta, M., & Garzanti, E. (2014). Which minerals control the Nd-Hf-Sr-Pb isotopic compositions of river sediments? *Chemical Geology*, *364*, 42–55. https://doi.org/10.1016/j.chemgeo.2013.11.018

Gili, S., Gaiero, D. M., Goldstein, S. L., Chemale, F., Jweda, J., Kaplan, M. R., et al. (2017). Glacial/interglacial changes of Southern Hemisphere wind circulation from the geochemistry of South American dust. *Earth and Planetary Science Letters*, *469*, 98–109. https://doi.org/10.1016/j.epsl.2017.04.007

Ginoux, P., Prospero, J. M., Gill, T. E., Hsu, N. C., & Zhao, M. (2012). Global-scale attribution of anthropogenic and natural dust sources and their emission rates based on MODIS Deep Blue aerosol products. *Reviews of Geophysics*, *50*, RG3005. https://doi.org/10.1029/2012RG000388

Goudie, A. S., & Middleton, N. J. (2006). *Desert dust in the global system*. Heidelberg: Springer. https://doi.org/10.1007/3-540-32355-4

Grousset, F. E., & Biscaye, P. E. (2005). Tracing dust sources and transport patterns using Sr, Nd and Pb isotopes. *Chemical Geology*, *222*, 149–167. https://doi.org/10.1016/j.chemgeo.2005.05.006

Hemming, S. R., van de Flierdt, T., Goldstein, S. L., Franzese, A. M., Roy, M., Gastineau, G., & Landrot, G. (2007). Strontium isotope tracing of terrigenous sediment dispersal in the Antarctic Circumpolar Current: Implications for constraining frontal positions. *Geochemistry, Geophysics, Geosystems*, *8*, Q06N13. https://doi.org/10.1029/2006GC001441

Hoernle, K., White, J. D. L., van den Bogaard, P., Hauff, F., Coombs, D. S., Werner, R., et al. (2006). Cenozoic intraplate volcanism on New Zealand: Upwelling induced by lithospheric removal. *Earth and Planetary Science Letters*, *248*, 350–367. https://doi.org/10.1016/j.epsl.2006.06.001

Huangfu, Y., Essington, M. E., Hawkins, S. A., Walker, F. R., Schwartz, J. S., & Layton, A. C. (2020). Testing the sediment fingerprinting technique using the SIAR model with artificial sediment mixtures. *Journal of Soils and Sediments*, *20*, 1771–1781. https://doi.org/10.1007/s11368-019-02545-7

Jaccard, S. L., Hayes, C. T., Martínez-García, A., Hodell, D. A., Anderson, R. F., Sigman, D. M., & Haug, G. H. (2013). Two modes of change in Southern Ocean productivity over the past million years. *Science*, *339*, 1419–1423. https://doi.org/10.1126/science.1227545

Jickells, T. D., An, Z. S., Andersen, K. K., Baker, A. R., Bergametti, C., Brooks, N., et al. (2005). Global iron connections between desert dust, ocean biogeochemistry, and climate. *Science*, *308*, 67–71. https://doi.org/10.1126/science.1105959

Karydis, V. A., Kumar, P., Barahona, D., Sokolik, I. N., & Nenes, A. (2011). On the effect of dust particles on global cloud condensation nuclei and cloud droplet number. *Journal of Geophysical Research*, *116*, D23204. https://doi.org/10.1029/2011JD016283

Koffman, B. G., Goldstein, S. L., Winckler, G., Borunda, A., Kaplan, M. R., Bolge, L., et al. (2021). New Zealand as a source of mineral dust to the atmosphere and ocean. *Quaternary Science Reviews*, *251*, 106659. https://doi.org/10.1016/j.quascirev.2020.106659

Kok, J. F., Ridley, D. A., Zhou, Q., Miller, R. L., Zhao, C., Heald, C. L., et al. (2017). Smaller desert dust cooling effect estimated from analysis of dust size and abundance. *Nature Geoscience*, *10*, 274–278. https://doi.org/10.1038/ngeo2912

Kok, J. F., Ward, D. S., Mahowald, N. M., & Evan, A. T. (2018). Global and regional importance of the direct dust-climate feedback. *Nature Communications*, *9*, 241. https://doi.org/10.1038/s41467-017-02620-y

Lambert, F., Delmonte, B., Petit, J. R., Bigler, M., Kaufmann, P. R., Hutterli, M. A., et al. (2008). Dust - climate couplings over the past 800,000 years from the EPICA Dome C ice core. *Nature*, *452*, 616–619. https://doi.org/10.1038/nature06763

Lamy, F., Gersonde, R., Winckler, G., Esper, O., Jaeschke, A., Kuhn, G., et al. (2014). Increased dust deposition in the Pacific Southern Ocean during glacial periods. *Science*, *343*, 403–407. https://doi.org/10.1126/science.1245424

Li, F., Ginoux, P., & Ramaswamy, V. (2008). Distribution, transport, and deposition of mineral dust in the Southern Ocean and Antarctica: Contribution of major sources. *Journal of Geophysical Research: Atmospheres*, *113*, D10207. https://doi.org/10.1029/2007JD009190

Li, L., Mahowald, N. M., Miller, R. L., Pérez García-Pando, C., Klose, M., Hamilton, D. S., et al. (2021). Quantifying the range of the dust direct radiative effect due to source mineralogy uncertainty. *Atmospheric Chemistry and Physics*, *21*, 3973–4005. https://doi.org/10.5194/acp-21-3973-2021

Longman, J., Veres, D., Ersek, V., Phillips, D. L., Chauvel, C., & Tamas, C. G. (2018). Quantitative assessment of Pb sources in isotopic mixtures using a Bayesian mixing model. *Scientific Reports*, *8*, 1–16. https://doi.org/10.1038/s41598-018-24474-0

Loveley, M. R., Marcantonio, F., Wisler, M. M., Hertzberg, J. E., Schmidt, M. W., & Lyle, M. (2017). Millennial-scale iron fertilization of the eastern equatorial Pacific over the past 100,000 years. *Nature Geoscience*, *10*, 760–764. https://doi.org/10.1038/ngeo3024

Lunt, D. J., & Valdes, P. J. (2002). The modern dust cycle: Comparison of model results with observations and study of sensitivities. *Journal of Geophysical Research: Atmospheres*, *107*, 4669–4671. https://doi.org/10.1029/2002JD002316

Maher, B. A., Prospero, J. M., Mackie, D., Gaiero, D., Hesse, P. P., & Balkanski, Y. (2010). Global connections between aeolian dust, climate and ocean biogeochemistry at the present day and at the last glacial maximum. *Earth-Science Reviews*, *99*, 61–97. https://doi.org/10.1016/j.earscirev.2009.12.001

Mahowald, N., Albani, S., Kok, J. F., Engelstaeder, S., Scanza, R., Ward, D. S., & Flanner, M. G. (2014). The size distribution of desert dust aerosols and its impact on the Earth system. *Aeolian Research*, *15*, 53–71. https://doi.org/10.1016/j.aeolia.2013.09.002

Mahowald, N. M., Baker, A. R., Bergametti, G., Brooks, N., Duce, R. A., Jickells, T. D., et al. (2005). Atmospheric global dust cycle and iron inputs to the ocean. *Global Biogeochemical Cycles*, *19*, GB4025. https://doi.org/10.1029/2004GB002402

Mahowald, N. M., Hamilton, D. S., Mackey, K. R. M., Moore, J. K., Baker, A. R., Scanza, R. A., & Zhang, Y. (2018). Aerosol trace metal leaching and impacts on marine microorganisms. *Nature Communications*, *9*, 2614. https://doi.org/10.1038/s41467-018-04970-7

Martin, J. H. (1990). Glacial-interglacial CO_2 change: The Iron Hypothesis. *Paleoceanography*, *5*, 1–13. https://doi.org/10.1029/PA005i001p00001

Martínez-García, A., Rosell-Melé, A., Jaccard, S. L., Geibert, W., Sigman, D. M., & Haug, G. H. (2011). Southern Ocean dust–climate coupling over the past four million years. *Nature*, *476*, 312–315. https://doi.org/10.1038/nature10310

Martínez-García, A., Sigman, D. M., Ren, H., Anderson, R. F., Straub, M., Hodell, D. A., et al. (2014). Iron fertilization of the subantarctic ocean during the last ice age. *Science*, *343*, 1347–1350. https://doi.org/10.1126/science.1246848

Marx, S. K., McGowan, H. A., & Kamber, B. S. (2009). Long-range dust transport from eastern Australia: A proxy for Holocene aridity and ENSO-type climate variability. *Earth and Planetary Science Letters*, *282*, 167–177. https://doi.org/10.1016/j.epsl.2009.03.013

McGee, D., Winckler, G., Borunda, A., Serno, S., Anderson, R. F., Recasens, C., et al. (2016). Tracking eolian dust with helium and thorium: Impacts of grain size and provenance. *Geochimica et Cosmochimica Acta*, *175*, 47–67. https://doi.org/10.1016/j.gca.2015.11.023

McGowan, H., & Clark, A. (2008). Identification of dust transport pathways from Lake Eyre, Australia using Hysplit. *Atmospheric Environment*, *42*, 6915–6925. https://doi.org/10.1016/j.atmosenv.2008.05.053

McGowan, H. A., Kamber, B., McTainsh, G. H., & Marx, S. K. (2005). High resolution provenancing of long travelled dust deposited on the Southern Alps, New Zealand. *Geomorphology*, *69*, 208–221. https://doi.org/10.1016/j.geomorph.2005.01.005

McTainsh, G. H. (1989). Quaternary aeolian dust processes and sediments in the Australian region. *Quaternary Science Reviews*, *8*, 235–253. https://doi.org/10.1016/0277-3791(89)90039-5

Molina-Kescher, M., Frank, M., Tapia, R., Ronge, T. A., Nürnberg, D., & Tiedemann, R. (2016). Reduced admixture of North Atlantic Deep Water to the deep central South Pacific during the last two glacial periods. *Paleoceanography*, *31*, 651–668. https://doi.org/10.1002/2015PA002863

Moore, C. M., Mills, M. M., Arrigo, K. R., Berman-Frank, I., Bopp, L., Boyd, P. W., et al. (2013). Processes and patterns of oceanic nutrient limitation. *Nature Geoscience*, *6*, 701–710. https://doi.org/10.1038/ngeo1765

Neff, P. D., & Bertler, N. A. N. (2015). Trajectory modeling of modern dust transport to the Southern Ocean and Antarctica. *Journal of Geophysical Research: Atmospheres*, *120*, 9303–9322. https://doi.org/10.1002/2015JD023304

Pabortsava, K., Lampitt, R. S., Benson, J., Crowe, C., McLachlan, R., Le Moigne, F. A. C., et al. (2017). Carbon sequestration in the deep Atlantic enhanced by Saharan dust. *Nature Geoscience*, *10*, 189–194. https://doi.org/10.1038/ngeo2899

Painter, T. H., Barrett, A. P., Landry, C. C., Neff, J. C., Cassidy, M. P., Lawrence, C. R., et al. (2007). Impact of disturbed desert soils on duration of mountain snow cover. *Geophysical Research Letters*, *34*, L12502. https://doi.org/10.1029/2007GL030284

Parnell, A. C., Inger, R., Bearhop, S., Jackson, A. L., & Macleod, H. (2010). Source partitioning using stable isotopes: Coping with too much variation. *PLoS One*, *5*, e9672. https://doi.org/10.1371/journal.pone.0009672

Parnell, A. C., Phillips, D. L., Bearhop, S., Semmens, B. X., Ward, E. J., Moore, J. W., et al. (2013). Bayesian stable isotope mixing models. *Environmetrics*, *24*, 387. https://doi.org/10.1002/env.2221

Phillips, D. L., Inger, R., Bearhop, S., Jackson, A. L., Moore, J. W., Parnell, A. C., et al. (2014). Best practices for use of stable isotope mixing models in food web studies. *Canadian Journal of Zoology*, *92*, 823–835. https://doi.org/10.1139/cjz-2014-0127

Pichat, S., Abouchami, W., & Galer, S. J. G. (2014). Lead isotopes in the Eastern Equatorial Pacific record Quaternary migration of the South Westerlies. *Earth and Planetary Science Letters*, *388*, 293–305. https://doi.org/10.1016/j.epsl.2013.11.035

Prospero, J. M., Ginoux, P., Torres, O., Nicholson, S. E., & Gill, T. E. (2002). Environmental characterization of global sources of atmospheric soil dust identified with the NIMBUS 7 Total Ozone Mapping Spectrometer (TOMS) absorbing aerosol product. *Reviews of Geophysics*, *40*, 1002–1011. https://doi.org/10.1029/2000RG000095

Rackow, T., Wesche, C., Timmermann, R., Hellmer, H. H., Juricke, S., & Jung, T. (2017). A simulation of small to giant Antarctic iceberg evolution: Differential impact on climatology estimates. *Journal of Geophysical Research: Oceans*, *122*, 3170–3190. https://doi.org/10.1002/2016JC012513

Revel-Rolland, M., De Deckker, P., Delmonte, B., Hesse, P. P., Magee, J. W., Basile-Doelsch, I., et al. (2006). Eastern Australia: A possible source of dust in East Antarctica interglacial ice. *Earth and Planetary Science Letters*, *249*, 1–13. https://doi.org/10.1016/j.epsl.2006.06.028

Sarmiento, J. L., & Gruber, N. (2006). *Ocean biogeochemical dynamics*. Princeton, NJ: Princeton University Press.

Schleicher, N. J., Dong, S., Packman, H., Little, S. H., Ochoa Gonzalez, R., Najorka, J., et al. (2020). A global assessment of copper, zinc, and lead isotopes in mineral dust sources and aerosols. *Frontiers of Earth Science*, *8*, 167. https://doi.org/10.3389/feart.2020.00167

Schlitzer, R. (2019). *Ocean Data View*. Retrieved from https://odv.awi.de

Shao, Y., Klose, M., & Wyrwoll, K.-H. (2013). Recent global dust trend and connections to climate forcing. *Journal of Geophysical Research: Atmospheres*, *118*, 11107–11111. https://doi.org/10.1002/jgrd.50836

Shi, Z., Krom, M. D., Jickells, T. D., Bonneville, S., Carslaw, K. S., Mihalopoulos, N., et al. (2012). Impacts on iron solubility in the mineral dust by processes in the source region and the atmosphere: A review. *Aeolian Research*, *5*, 21–42. https://doi.org/10.1016/j.aeolia.2012.03.001

Shoenfelt, E. M., Winckler, G., Lamy, F., Anderson, R. F., & Bostick, B. C. (2018). Highly bioavailable dust-borne iron delivered to the Southern Ocean during glacial periods. *Proceedings of the National Academy of Sciences of the United States of America*, *115*, 11180–11185. https://doi.org/10.1073/pnas.1809755115

Sigman, D. M., & Boyle, E. A. (2000). Glacial/interglacial variations in atmospheric carbon dioxide. *Nature*, *407*, 859–869. https://doi.org/10.1038/35038000

Simões Pereira, P., van de Flierdt, T., Hemming, S. R., Hammond, S. J., Kuhn, G., Brachfeld, S., et al. (2018). Geochemical fingerprints of glacially eroded bedrock from West Antarctica: Detrital thermochronology, radiogenic isotope systematics and trace element geochemistry in Late Holocene glacial-marine sediments. *Earth-Science Reviews*, *182*, 204–232. https://doi.org/10.1016/J.EARSCIREV.2018.04.011

Smetacek, V., Klaas, C., Strass, V. H., Assmy, P., Montresor, M., Cisewski, B., et al. (2012). Deep carbon export from a Southern Ocean iron-fertilized diatom bloom. *Nature*, *487*, 313–319. https://doi.org/10.1038/nature11229

Souto-Oliveira, C. E., Babinski, M., Araújo, D. F., & Andrade, M. F. (2018). Multi-isotopic fingerprints (Pb, Zn, Cu) applied for urban aerosol source apportionment and discrimination. The *Science of the Total Environment*, *626*, 1350–1366. https://doi.org/10.1016/j.scitotenv.2018.01.192

Stock, B., & Semmens, B. (2013). *MixSIAR GUI user manual*. https://doi.org/10.5281/zenodo.47719. Version 3.1

Stock, B. C., Jackson, A. L., Ward, E. J., Parnell, A. C., Phillips, D. L., & Semmens, B. X. (2018). Analyzing mixing systems using a new generation of Bayesian tracer mixing models. *PeerJ*, *6*, e5096. https://doi.org/10.7717/peerj.5096

Struve, T., Pahnke, K., Lamy, F., Wengler, M., Böning, P., & Winckler, G. (2020). A circumpolar dust conveyor in the glacial Southern Ocean. *Nature Communications*, *11*, 5655. https://doi.org/10.1038/s41467-020-18858-y

Tagliabue, A., Bowie, A. R., Boyd, P. W., Buck, K. N., Johnson, K. S., & Saito, M. A. (2017). The integral role of iron in ocean biogeochemistry. *Nature*, *543*, 51–59. https://doi.org/10.1038/nature21058

Trudgill, M. D., Shuttleworth, R., Bostock, H. C., Burke, A., Cooper, M. J., Greenop, R., & Foster, G. L. (2020). The flux and provenance of dust delivered to the SW Pacific during the last glacial maximum. *Paleoceanography and Paleoclimatology*, *35*, e2020PA003869. https://doi.org/10.1029/2020PA003869

Uno, I., Eguchi, K., Yumimoto, K., Takemura, T., Shimizu, A., Uematsu, M., et al. (2009). Asian dust transported one full circuit around the globe. *Nature Geoscience*, *2*, 557–560. https://doi.org/10.1038/ngeo583

van der Does, M., Wengler, M., Lamy, F., Martínez-García, A., Jaccard, S. L., Kuhn, G., & Winckler, G. (2021). Opposite dust grain-size patterns in the Pacific and Atlantic sectors of the Southern Ocean during the last 260,000 years. *Quaternary science reviews*, *263*, 106978. https://doi.org/10.1016/j.quascirev.2021.106978

Wengler, M., Lamy, F., Struve, T., Borunda, A., Böning, P., Geibert, W., et al. (2019). A geochemical approach to reconstruct modern dust fluxes and sources to the South Pacific. *Geochimica et Cosmochimica Acta*, *264*, 205–223. https://doi.org/10.1016/j.gca.2019.08.024

Winton, V. H. L., Dunbar, G. B., Bertler, N. A. N., Millet, M.-A., Delmonte, B., Atkins, C. B., et al. (2014). The contribution of aeolian sand and dust to iron fertilization of phytoplankton blooms in southwestern Ross Sea, Antarctica. *Global Biogeochemical Cycles*, *28*, 423–436. https://doi.org/10.1002/2013GB004574

Wu, Y., Roberts, A. P., Grant, K. M., Heslop, D., Pillans, B. J., Zhao, X., et al. (2021). Climatically modulated dust inputs from New Zealand to the Southwest Pacific sector of the Southern Ocean over the last 410 kyr. *Paleoceanography and Paleoclimatology*, *36*, e2020PA003949. https://doi.org/10.1029/2020PA003949

Yang, X., Liu, Y., Li, C., Song, Y., Zhu, H., & Jin, X. (2007). Rare earth elements of aeolian deposits in Northern China and their implications for determining the provenance of dust storms in Beijing. *Geomorphology*, *87*, 365–377. https://doi.org/10.1016/j.geomorph.2006.10.004